

Oceanic spreading ridge
Triple junction
Indian Ocean

Dorsale médio-océanique
Point triple
Océan Indien

The Rodriguez Triple Junction (Indian Ocean) : Structure and Evolution for the Past One Million Years*

Marc MUNSCHY, Roland SCHLICH

Institut de Physique du Globe, Laboratoire de Géophysique Marine (CNRS UA 323), 67084
Strasbourg Cedex, France

*This article has been previously published in : *Marine Geophysical Researches* 11 : 1-14, 1989.
© 1989 Kluwer Academic Publishers. Printed in the Netherlands.

ABSTRACT

The Rodriguez Triple Junction (RTJ) corresponds to the junction of the three Indian Ocean spreading ridges. A detailed survey of an area of 90 km by 85 km, centered at 25°30'S and 70°E, allows detailed mapping (at a scale of 1/100 000) of the bathymetry (Seabeam) and the magnetic anomalies. The Southeast Indian Ridge, close to the triple junction, is a typical intermediate spreading rate ridge (2.99 cm a⁻¹ half rate) trending N140°. The Central Indian Ridge rift valley prolongs the Southeast Indian Ridge rift valley with a slight change of orientation (12°). The half spreading rate and trend of this ridge are 2.73 cm a⁻¹ and N152° respectively. In contrast, the Southwest Indian Ridge close to the triple junction is expressed by two deep-valleys (4300 and 5000 m deep) which abut the southwestern flanks of the two other ridges, and appears to be a stretched area without axial neovolcanic zone. The evolution of the RTJ is analysed for the past one million years. The instantaneous velocity triangle formed by the three ridges cannot be closed indicating that the RTJ is unstable. A model is proposed to explain the evolution of the unstable RRF Rodriguez Triple Junction. The model shows that the axis of the Central Indian Ridge is progressively offset from the axis of the Southeast Indian Ridge at a velocity of 0.14 cm a⁻¹, the RTJ being restored by small jumps. This unstable RRF model explains the directions and offsets which are observed in the vicinity of the triple junction. The structure and evolution of the RTJ is similar to that of the Galapagos Triple Junction located in the East Pacific Ocean and the Azores Triple Junction located in the Central Atlantic Ocean.

Oceanologica Acta, 1990. Volume spécial 10, Actes du Colloque Tour du Monde Jean Charcot, 2-3 mars 1989, Paris. 129-142.

RÉSUMÉ

Le point de Rodriguez (Océan Indien) : structure et évolution au cours du dernier million d'années

Le point triple de Rodriguez correspond au point de jonction des trois dorsales actives de l'Océan Indien. Un levé systématique, bathymétrique (Seabeam) et magnétique (champ total), d'une zone de 90 sur 85 km, centrée sur 25°30'S et 70°E, permet de dresser un ensemble de cartes détaillées à l'échelle de 1/100 000ème pour toute la zone du point triple de Rodriguez. La dorsale est-indienne, à proximité du point triple, correspond à une dorsale intermédiaire (2,99 cm/a pour le taux d'expansion), orientée N 140°. La dorsale centrale-

indienne prolonge vers le nord, après un léger changement d'orientation (12°), la dorsale est-indienne. Le taux d'expansion et la direction de cette dorsale sont de $2,73 \text{ cm/a}$ et $N 152^\circ$. La dorsale ouest-indienne à proximité du point triple, n'est exprimée que par deux profondes déchirures (4 300 et 5 000 m), sans structure volcanique apparente, distantes de 7 km et de direction $N 067^\circ$.

L'évolution du point triple de Rodriguez est analysée pour le dernier million d'années. Le triangle de vitesse formé par les trois dorsales n'est pas fermé, ce qui implique l'instabilité du point triple correspondant. Le modèle proposé montre que l'axe de la dorsale centrale-indienne se décale progressivement par rapport à l'axe de la dorsale est-indienne, à une vitesse de l'ordre de $0,14 \text{ cm/a}$; la jonction triple est rétablie par sauts du point triple. Ce modèle instable, de type RRF, explique l'ensemble des directions et décalages mesurés à proximité du point triple, et rend compte des reliefs observés. La structure et l'évolution du point triple de Rodriguez ressemblent à celles du point triple des Galapagos dans l'Océan Pacifique Est, et à celles du point triple des Açores dans l'Océan Atlantique central.

Oceanologica Acta, 1990. Volume spécial 10, Actes du Colloque Tour du Monde Jean Charcot, 2-3 mars 1989, Paris, 129-142.

INTRODUCTION

The topography of the Indian Ocean is dominated by a system of three oceanic spreading ridges converging at the Rodriguez Triple Junction (RTJ), located near $25^\circ 30' S$ and $70^\circ E$, 900 km southwestward from the Rodriguez Island (Fig. 1). Numerous studies have been carried out on these three ridges and were synthesized by Schlich (1982).

The Southeast Indian Ridge (SEIR), the boundary between the Antarctica and Australian plates, extends southeastward from the RTJ through the island of Amsterdam and Saint-Paul and joins the Pacific-Antarctic Ridge at the Macquarie Ridge Complex south of Australia. The half spreading rate and ridge trend close to the RTJ are known to be 3.0 cm a^{-1} and $N137^\circ$ respectively (Tapscott *et al.*, 1980) and to progressively change to 3.7 cm a^{-1} and $N094^\circ$ at the Macquarie Ridge Complex (Weissel and Hayes, 1972). The SEIR morphology is typical of an intermediate spreading rate ridge (Macdonald, 1982) with a smooth relief and a 100-300 m deep rift valley extending from the RTJ to the islands of Amsterdam and Saint-Paul (Royer, 1985). The Central Indian Ridge (CIR), the boundary between the African and Indian plates, extends north of the RTJ towards the equator where it reaches the southern end of the Carlsberg Ridge. The half spreading rate and ridge trend progressively change between the RTJ and the equator from 2.5 cm a^{-1} and $N149^\circ$ (Tapscott *et al.*, 1980) to 1.8 cm a^{-1} and $N142^\circ$ (Fisher *et al.*, 1971). The morphology of the CIR is slightly more rugged compared to the SEIR. The Southwest Indian Ridge (SWIR), the boundary between the African and Antarctic plates, extends between the RTJ and the Bouvet Triple Junction ($55^\circ S$ and $01^\circ W$); the ridge axis trends $N090^\circ$ at the RTJ (Tapscott *et al.*, 1980) and changes to $N135^\circ$ at the Bouvet Triple Junction (Sclater *et al.*, 1976). The half spreading rate is almost constant along the SWIR (0.8 cm a^{-1}). The topography of the SWIR is extremely rugged with a 1000-

3000 m deep rift valley. This morphology is typical of the slow spreading rate ridges (Macdonald, 1982).

The existence of the RTJ was first discussed by McKenzie and Sclater (1971). Tapscott *et al.* (1980) have analysed the data collected by the R/V *Atlantis II*, cruise 93 legs 5 and 6 (1976), within a distance of 250 km from the triple junction. They defined the half spreading rates and trends for the three ridges: 3.0 cm a^{-1} and $N137^\circ$ for the SEIR, 2.5 cm a^{-1} and $N149^\circ$ for the CIR, and 0.8 cm a^{-1} and $N090^\circ$ for the SWIR. They located the triple junction to within 5 km at $25^\circ 40' S$ and $70^\circ 06' E$ and concluded that the RTJ is a stable ridge-ridge-ridge (RRR) triple junction. On the other hand, Patriat and Courtillot (1984) have suggested that the RTJ evolves in two preferred modes of 1 Ma duration.

The RTJ has been surveyed in February (cruise Rodriguez I) and April (cruise Rodriguez II) 1984 by the R/V *Jean Charcot* (Schlich *et al.*, 1987). The survey comprises 4150 km of profiles covering some 7600 km² and is centered on the RTJ. The bathymetry was acquired with a multi-narrow-beam echo sounder (from General Instrument Corporation) and corresponds to individual isobath swaths on the seafloor; the width of the swaths is 3/4 of the water depth (Renard and Allenou, 1979). Considering the spacing of the profiles the area is completely covered by the swaths. The most detailed data are Seabeam swaths at a scale of 1/25 000 with a 20 m contour interval which can resolve small scale features such as isolated volcanoes. Gravimetric and magnetic data were continuously recorded along the Seabeam tracks.

In this paper we use the new bathymetric and magnetic charts to analyse the characteristics of the three ridges close to the RTJ, and to examine the concept of rigidity of tectonic plates at this scale. We also examine the evolution of the RTJ during the past one million years and suggest an unstable RRF model which is consistent with the detailed geophysical data collected over this region.

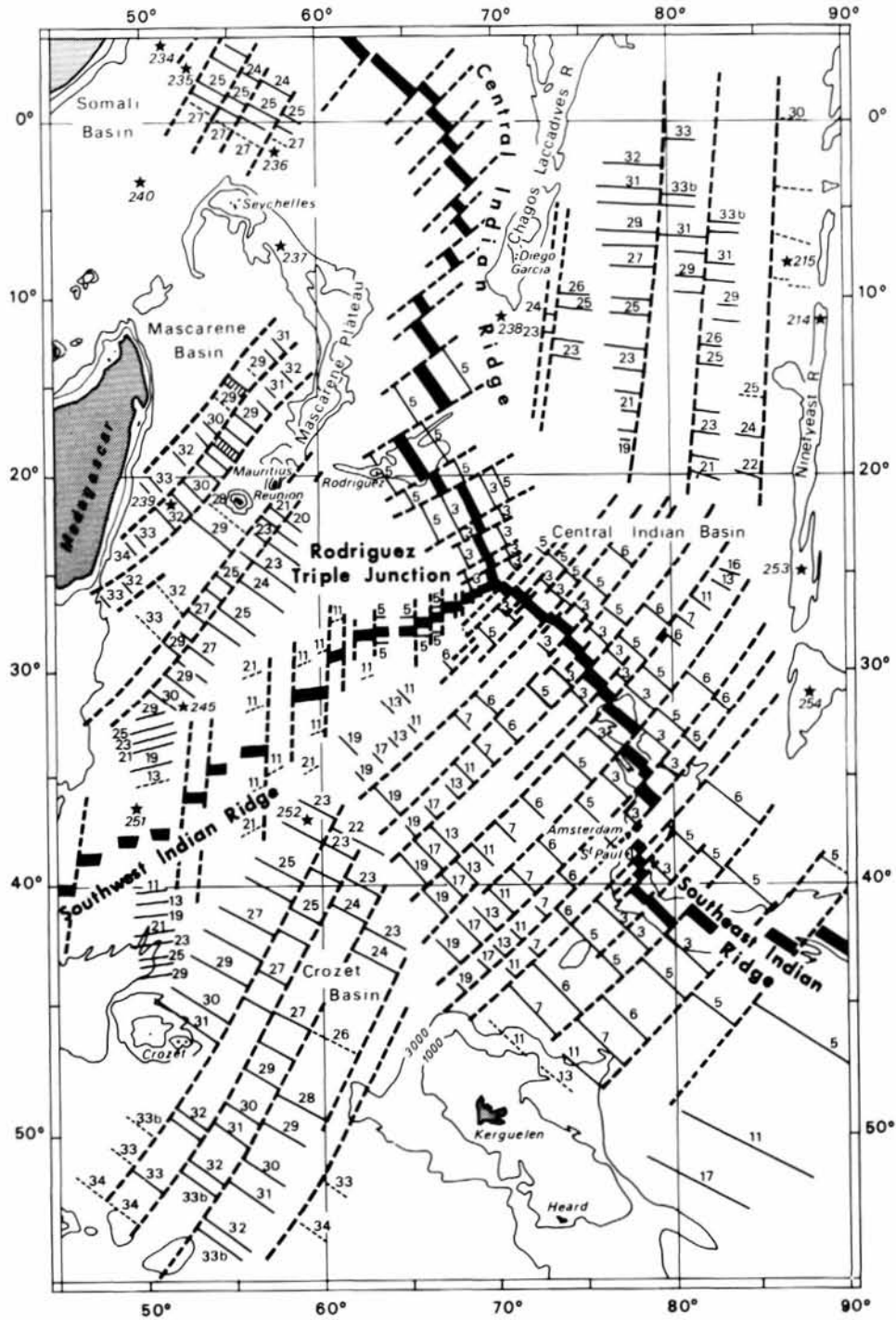
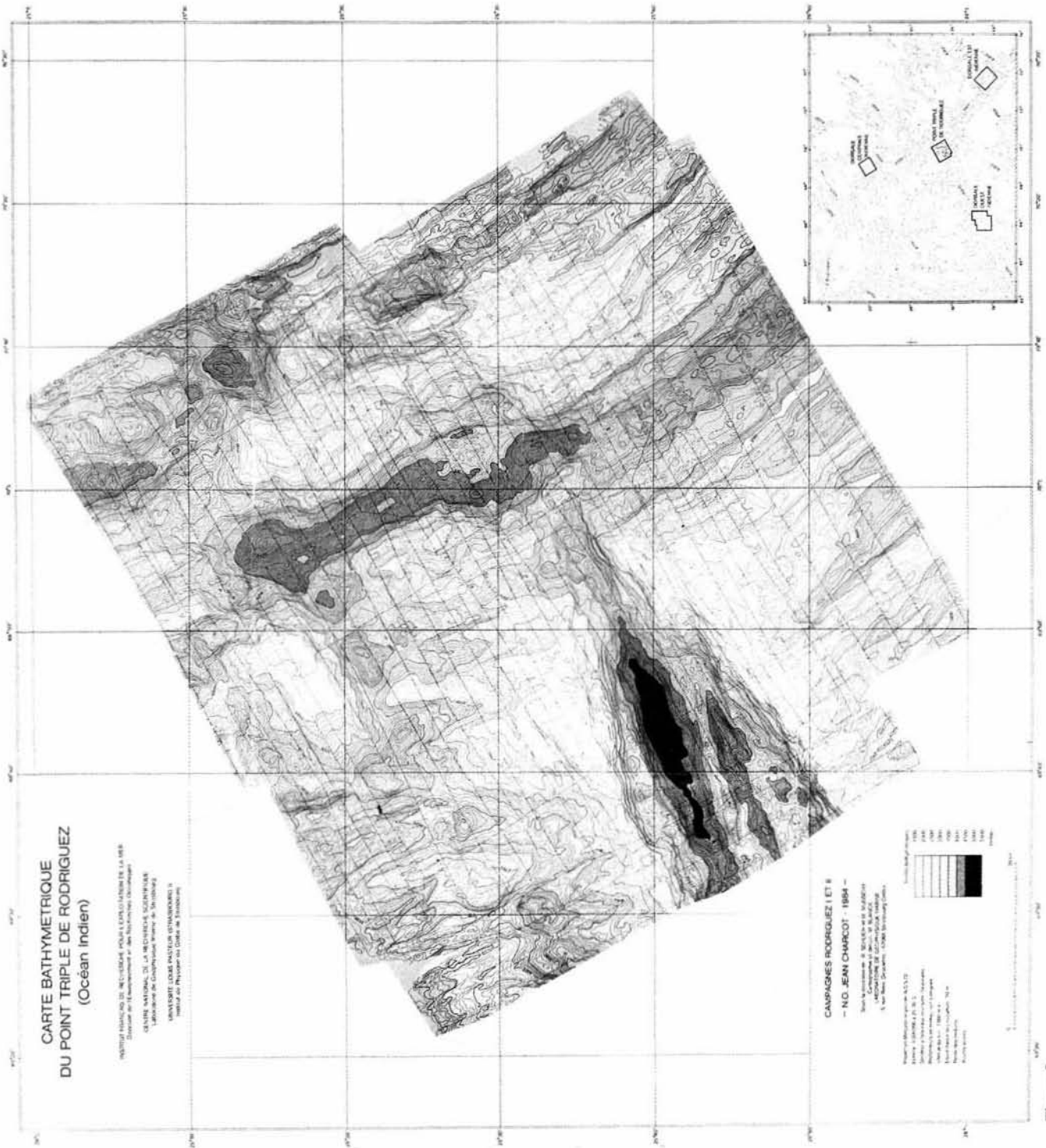


Figure 1

Fracture zones and magnetic lineations in the Indian Ocean superimposed on the 1000 and 3000 m bathymetric contour (Schlich, 1982; Royer, 1985; Munsch, 1987). The fracture zone are indicated by dashed lines; the magnetic lineations are shown by solid lines or dotted lines if questionable; the numbers follow the magnetic time scale proposed by Lowrie and Alvarez (1981); DSDP sites are starred and located by their numbers.



Bathymetric chart of the Rodriguez Triple Junction. Contour interval is 50 m, colour changes every 500 m. R/V Jean Charcot tracks are shown by dotted lines.

BATHYMETRY

Conventional Transit Satellite navigation has been used for the survey. Comparison of the Seabeam swaths at 50 m contour interval at the 132 crossing points allow us to readjust the original satellite navigation by coherent relative displacement of the individual lines. Thus, a more accurate geographic position has been defined for each crossing point and a new navigation was computed. The differences of water depth observed at the 132 crossing points before and after the readjustment of the navigation indicate that the relative position of the lines is probably better than 300 m (Munsch, 1987); the relative precision of the original satellite-based navigation is only 2 km. The RTJ bathymetric chart has been drawn with a 50 m contour interval at the scale of 1/100 000 and 1/200 000 (Schlich *et al.*, 1988). The colour chart at the scale of 1/200 000 is shown in Figure 2.

On the bathymetric chart (Fig. 2) the triple junction corresponds to a 50 km² area centered at 25°32'S and 70°02'E. The characteristics of the three ridges and the location of the triple junction traces on each of the three tectonic plates are well constrained.

The segment of the SEIR covered by the bathymetric chart is about 30 km long. This segment of the SEIR corresponds to a typical intermediate spreading rate ridge (Macdonald, 1982). The topography of the flanks is relatively smooth with reliefs of 100-400 m and the ridge appears grossly symmetric (Fig. 3). The rift valley is 200-600 m

deep, 15-20 km wide and is usually well defined. The inner floor, 4 km wide, is flat along and across the axis, and lies at a depth about 3600 m. The main normal faults and bathymetric lineaments appear very continuous along strike and have been mapped on both flanks of the ridge (Fig. 4). These structural elements are striking at N140.3° ($\pm 3.7^\circ$) along the northeastern flank and N139.8° ($\pm 3.3^\circ$) along the southwestern flank. The scattering of the directions is very low and appears to be associated with measurement errors. Finally, the direction of the SEIR, deduced from the bathymetric elements, appears very uniform close to the RTJ and is trending N140°.

The CIR rift valley prolongs the SEIR rift valley with a slight change of orientation (12°) and an offset of about 5 km. Close to the northern limit of the bathymetric chart, the CIR is offset 14 km to the northeast by a transform fault trending N061° (Fig. 4). between the RTJ and this transform fault the CIR rift valley is formed by two segments, 18 and 10 km long, showing a dextrally offset of 4 km between them. The CIR rift valley is deeper (600-1000 m) than the SEIR rift valley. The inner floor, 2-4 km wide, is flat and its depth (about 4000 m) is 400 m deeper than the SEIR inner floor (Fig. 3). Compared to the SEIR, the structure of the CIR is more rugged and variable. Particularly, the throws on the normal faults are larger and the lineaments are shorter. The direction of the lineaments, measured on the northeastern and southwestern flanks of the CIR, are N150.8° ($\pm 3.2^\circ$) and N153.8° ($\pm 5.4^\circ$) respectively. This difference between the two flanks is not significant and the direction of the CIR close to the RTJ appears uniform at N152°.

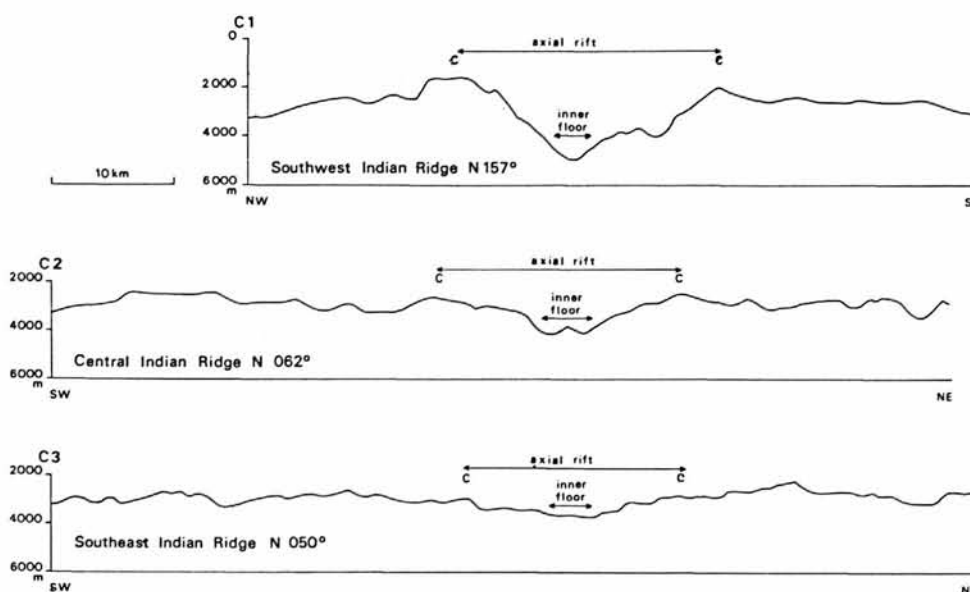


Figure 3

Line drawings across the Southwest India Ridge (C1), the Central Indian Ridge (C2) and the Southeast Indian Ridge (C3). The location of the profiles is shown on Figure 4.

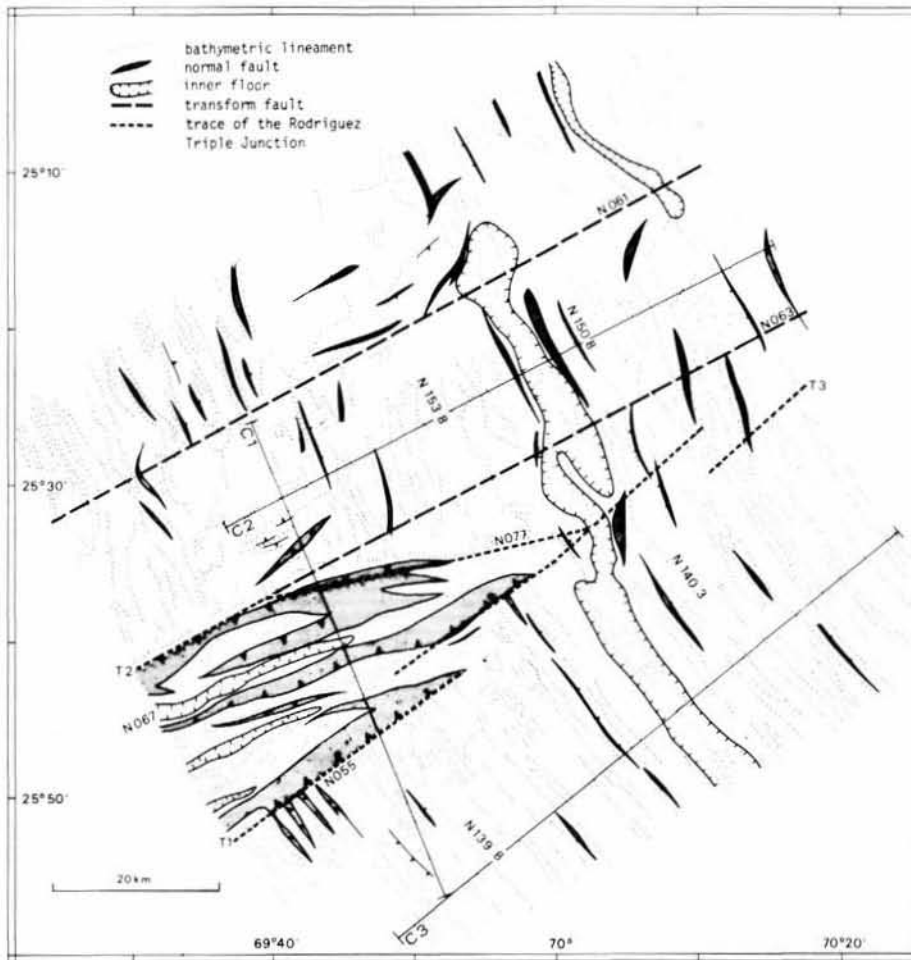


Figure 4

Tectonic elements of the Rodriguez Triple Junction deduced from the bathymetric chart. Lines C1, C2, C3 mark the position of the line drawings of Figure 3.

In contrast the SWIR has an extreme relief and is expressed by two narrow, V-shaped deep-valleys (5000 and 4300 m deep), lying 7 km apart (Fig. 4). Their floors are very narrow (about 500 m). The trend of these two deep-valleys remains constant within the surveyed area and their mean direction is N067°. The flanks of the valleys are extremely steep (45°) and correspond to major normal faults (Fig. 3). The shape of these tectonic features suggests that the deep-valleys are the result of stretching along the southwestern flanks of the SEIR and CIR.

The three traces of the RTJ are the sutures between the crust created at the corresponding ridges on each of the three tectonic plates. The trace of the RTJ between the SEIR and SWIR (on the Antarctic Plate, T1) is one of the major features observed on the bathymetric chart (Fig. 2). The strike of the lineations changes by about 90° over a distance of about 200 m. Moreover this zone is linear and trends N055°. At a distance of about 15 km from the RTJ, the trace is offset 5 km to the south (Fig. 4). The trace of the RTJ between the CIR and SWIR (on the African Plate, T2) is also well expressed. The shift of the topographic lineations occurs over a distance of about

500 m. The strike of this trace is N077° between the RTJ and 40 km away. At this distance the trace corresponds to the fracture zone between the two segments of the CIR and trends N063° (Fig. 4). In contrast, the trace of the RTJ between the SEIR and CIR (on the Indian Plate, T3) is poorly expressed on the bathymetric chart but can be determined from the distribution of the bathymetric lineaments. The trace T3 corresponds to a zone larger than 5 km where the bathymetric lineaments are interrupted.

MAGNETIZATION AND HALF SPREADING RATES

The temporal variation of the geomagnetic field at the RTJ was reconstructed for the period of time corresponding to the survey by using a regression technique (Sander and Mrazek, 1982) and the total field values measured at the different crossing points. The temporal variation obtained shows a strong similarity with the tem-

poral variation recorded at the Martin de Vivies Magnetic Observatory (Amsterdam Island) located 1500 km south-eastward from the RTJ (Fig. 5). The computed temporal variation was removed from the total field measurements and the final RMS for the crossover errors was reduced

to 4.2 nT; the RMS for the original satellite-based navigation was 15.2 nT. Finally the International Reference Geomagnetic Field (Peddie, 1982) was subtracted from these reduced total field measurements to obtain the magnetic anomaly field (Fig. 6).

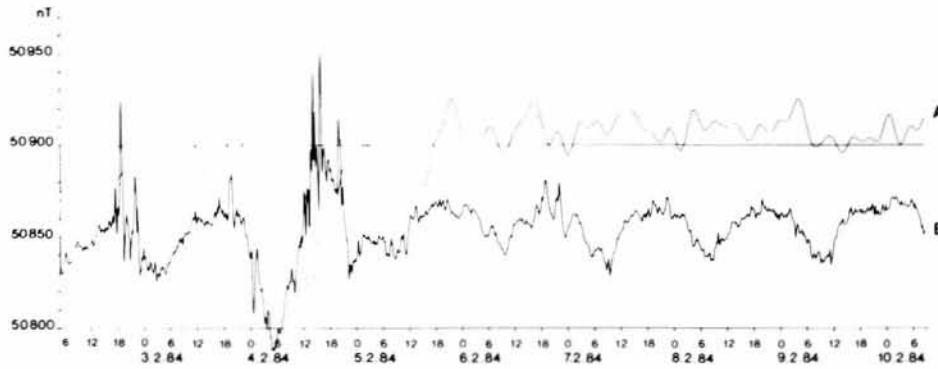


Figure 5

Comparison of the temporal variation of the magnetic field computed during the survey on the Rodriguez Triple Junction (A) with the temporal variation recorded at the Martin de Vivies Magnetic observatory on Amsterdam Island (B).

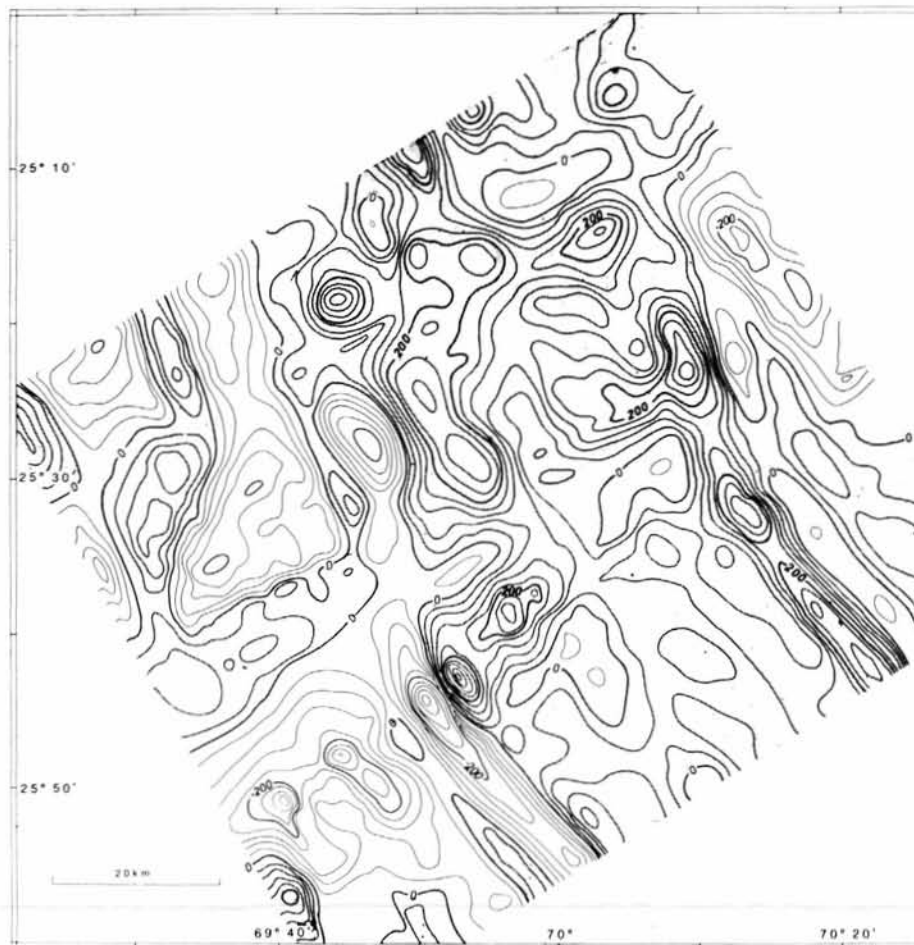


Figure 6

Magnetic anomaly field over the Rodriguez Triple Junction. Positive anomalies are shaded. The contour interval is 40 nT.

The bathymetry and the magnetic anomaly field were digitized and gridded using linear interpolation. The gridded data form a 57×57 array with a spacing of 2 km. The gridded magnetic field was then inverted in the presence of bathymetry using the method of Parker and Huestis (1974) extended to three dimensions by Macdonald *et al.* (1980). The magnetized crust is assumed to be a layer of constant thickness (500 m) which follows the bathymetry and with constant magnetization with depth. To prevent the oscillation of the solution at short wavelength, the magnetization was low-pass filtered at each iteration with a cosine taper between 5.3 and 4.8 km. The magnetization distribution (Fig. 7) is given in amperes per meter ($1 \text{ A m}^{-1} = 10^{-3}$). The maximum deviation between the computed field from the solution and the observed field is less than 20 nT.

Along the axial zone of the SEIR and CIR the magnetization is positive (about $3\text{--}5 \text{ A m}^{-1}$). Along each flank of the SEIR and CIR, three positive/negative magnetized boundaries are visible, but are not apparent on the SWIR. These boundaries mark crustal isochrons which recorded the three most recent inversions of the magnetic field. Using the magnetic time scale of Lowrie and Alvarez (1981), these three isochrons are dated at 0.72 Ma

(Brunhes/Matuyama reversal), 0.91 Ma (Matuyama/Jaramillo reversal) and 0.97 Ma (Jaramillo/Matuyama reversal). The observed trends of the isochrons are in remarkable agreement with the trends of the corresponding bathymetric lineaments. The transition width, defined as the distance between the 90% levels of full positive and negative polarity (Atwater and Mudie, 1983), is about 2 km for the Brunhes/Matuyama reversal on the SEIR and CIR. This transition width is equal to the spacing of the gridded data (2 km) indicating that this value may be overestimated, due to the coarseness of the gridding and the smoothing required to obtain a stable solution for the magnetization.

The first two isochrons were used to compute the half spreading rates for the SEIR and CIR. Along the SEIR the values obtained are $2.99 \pm 0.07 \text{ cm a}^{-1}$ between 0 and 0.72 Ma, $3.35 \pm 0.47 \text{ cm a}^{-1}$ between 0.72 and 0.91 Ma on the northeastern flank, and $2.66 \pm 0.38 \text{ cm a}^{-1}$ between 0.72 and 0.91 Ma on the southwestern flank of the ridge. These values remain constant along the axis with no asymmetry of direction. The differences in half spreading rate between the northeastern and the southwestern flanks during the second period is significant (0.69 cm a^{-1}), but the mean half spreading rate of 3.01 cm a^{-1} for this period



Figure 7

Magnetization distribution over the Rodriguez Triple Junction contoured in amperes per meter (contour interval 2 A m^{-1}). Positive magnetized zones are shaded.

is the same as the computed 2.99 cm a^{-1} for the first period. Thus, the SEIR has been spreading at a half rate of 2.99 cm a^{-1} since 0.91 Ma. During the second period, between 0.72 and 0.91 Ma, the northeastern flank is 1.4 km larger than the southwestern flank; this difference could correspond to an instantaneous 0.7 km jump of the ridge axis towards the southwest or to a continuous migration of the ridge axis at a velocity of 0.35 cm a^{-1} towards the southwest. The data available do not allow to favour one or the other possibility.

Along the CIR the half spreading rates are $2.73 \pm 0.03 \text{ cm a}^{-1}$ between 0 and 0.72 Ma, $2.61 \pm 0.39 \text{ cm a}^{-1}$ between 0.72 and 0.91 Ma on the northeastern flank and $2.84 \pm 0.33 \text{ cm a}^{-1}$ between 0.72 and 0.91 Ma on the southwestern flank. The mean half spreading rate of 2.73 cm a^{-1} for the second period is the same than for the first period. Thus, the CIR has been spreading at a half rate of 2.73 cm a^{-1} since 0.91 Ma. As suggested for the SEIR, the asymmetric spreading during the second period may be related to a 0.2 km jump of the axis to the northeastern or to a continuous asymmetric expansion of the CIR.

EVOLUTION OF THE RODRIGUEZ TRIPLE JUNCTION FOR THE PAST ONE MILLION YEARS

Knowing the directions and the spreading rate of the three ridges, as well as the directions and the shapes of the RTJ traces on the three plates, different models of evolution of the RTJ can be built for the past one million years. These models assume that the three tectonic plates remain rigid close to the RTJ. This assumption cannot be

completely confirmed, but the computed mean values for the directions and spreading rates of the SEIR and CIR do not indicate deformation of the tectonic plates. In the same way, the detailed bathymetry along the three traces of the RTJ gives no evidence of intraplate deformation.

Stable RRR triple junction model

The RTJ is a RRR junction for the last 80 Ma (Schlich, 1982) and appears to be stable in the sense of McKenzie and Morgan (1969), as discussed by Tapscott *et al.* (1980). The precise directions and the new spreading rate values which were determined for the SEIR and CIR, can be used to check if the two ridges are spreading symmetrical at right angles to their strikes. The half spreading rates obtained for the SEIR and CIR show that the asymmetry of spreading is not large; only 11 % for the SEIR and 6 % for the CIR from 0.72 to 0.91 Ma. The trend of the transform fault offsetting the CIR at the northern end of the bathymetric chart (N061°) was obtained by averaging the directions of the normal faults and bathymetric lineaments associated with this transform fault. The mean direction is at right angles to the N152° strike of the CIR. Along the SEIR segment covered by the survey, no transform fault is visible, but Tapscott *et al.* (1980) have suggested that, close to the RTJ, the SEIR is spreading symmetrically in a direction normal to its strike.

A stability diagram of the RTJ can be constructed using the velocity triangle (McKenzie and Morgan, 1969) and assuming a RRR mode. The half spreading rate and the direction of both the SEIR and the CIR form two sides of the triangle (Figure 8a); the third side of the triangle gives the direction and half spreading rate of the SWIR. The values obtained are respectively N078° and 0.65 cm a^{-1} . Based on these directions and spreading rates, an

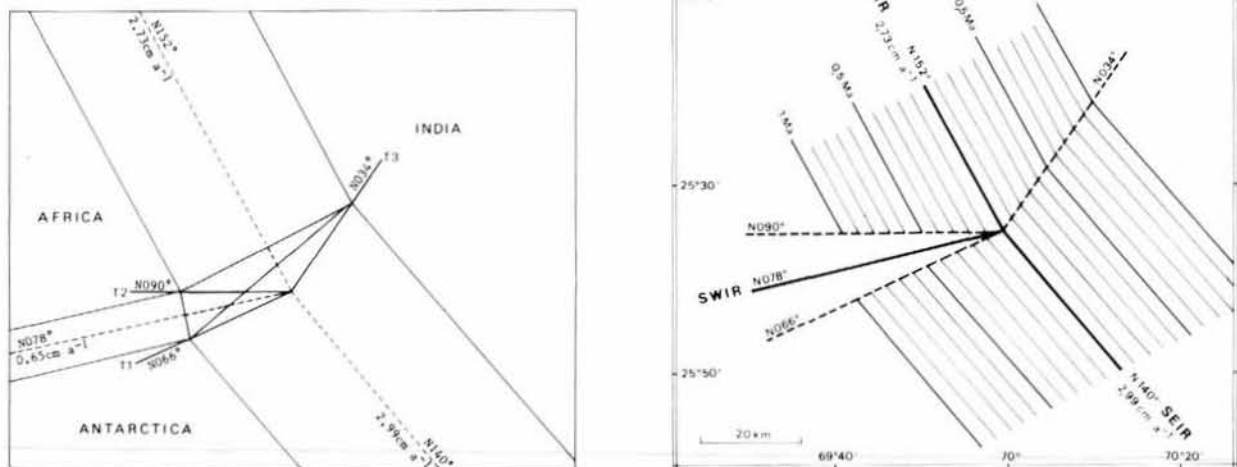


Figure 8

a - Present velocity triangle for the Rodriguez Triple Junction following the representation of Patriat and Courtillot (1984) : stable RRR model.
 b - Schematic isochron pattern obtained with the stable RRR configuration of the Rodriguez Triple Junction. The isochrons are at 0.1 Ma intervals.

isochron pattern of the RTJ has been drawn (Figure 8b). The morphostructural map (Figure 9), deduced from the tectonic map (Figure 4) and from the isochron pattern of the magnetization map (Figure 7) is compared to the isochron pattern produced by the evolving stable triple junction model (Figure 8b). The directions computed for the traces of the RTJ on the Antarctic Plate (RTJ trace T1), on the African Plate (RTJ trace T2) and the spreading direction of the SWIR (respectively N066°, N090° and N078°) are quite different from those observed on the morphostructural map (N055°, N077° and N067°), especially for the direction of the RTJ trace T1 and for the direction of the deep-valleys which are clear on the morphostructural map (Figure 9). The model does not account for the offset between the SEIR and CIR rift valleys. Moreover the model predicts that the SEIR would presently be receding at 0.76 cm a⁻¹, while it has been observed that the SEIR has remained almost constant in length since the Late Cretaceous (Schlich, 1982 and Figure 1).

Thus, a stable RRR model as proposed by Tapscott *et al.* (1980) on the basis of their study of the magnetic lineations and spreading directions of the three ridges since 10 Ma, is not consistent with the more detailed directions observed on the new bathymetric chart of the RTJ.

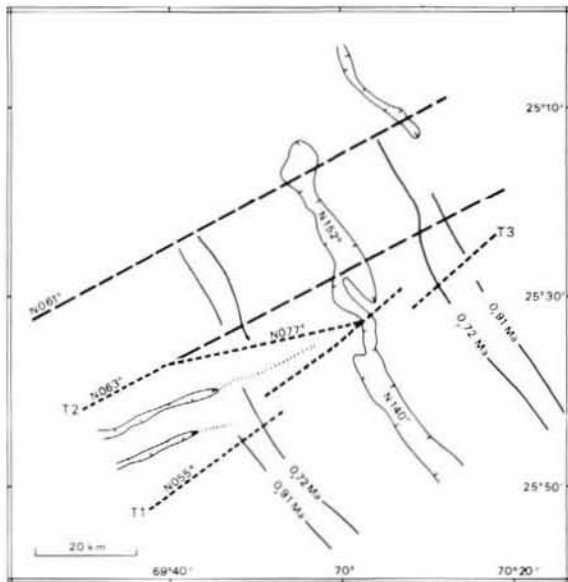


Figure 9

Schematic morphostructural map of the Rodriguez Triple Junction deduced from the tectonic map (Fig. 4) and from the isochrons pattern of the magnetization map (Fig. 7).

Unstable RRF triple junction model

The trace T1 is a major feature on the bathymetric chart of the RTJ and therefore should clearly appear on the final model of evolution. Thus, we consider a model based on this N055° direction. The velocity triangle is formed by the directions and spreading rates of the SEIR and the CIR; we impose the direction of the RTJ trace T1 as to be equal to N055°. Assuming that the spreading of the

SEIR and CIR is symmetric and at right angles to the strike of the ridges, we obtain the direction of the RTJ trace T3 (N045°), the direction of the RTJ trace T2 (N079°) and the direction of the SWIR (N067°). The direction of the SWIR corresponds to the mean between the directions of the RTJ traces T1 and T2, if the SWIR is spreading symmetrically (Figure 10a). The directions obtained for the SWIR and for the RTJ trace T2 are the same as the directions observed for the deep-valleys (N067°) and for the RTJ trace T2 (N077°) as shown on Figure 9. Thus, all the directions given by the model are equal to those observed and the half spreading rate of 0.65 cm a⁻¹ obtained for the SWIR is unchanged. This model is unstable : the CIR and SEIR axis are progressively offset at a velocity of 0.14 cm a⁻¹, and as a result the RTJ evolves in a segment of increasing length (Figure 10b). This evolution is recorded by the offsets between the corresponding

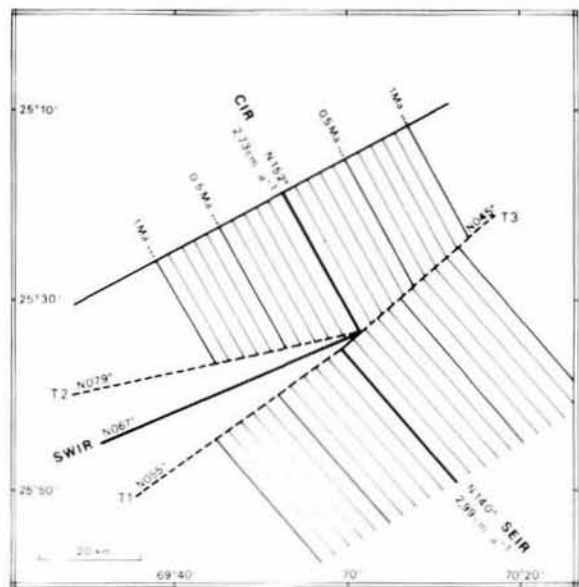
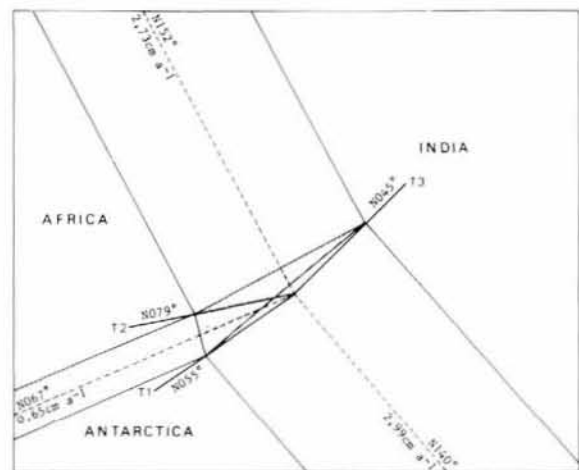


Figure 10

a - Present velocity triangle for the Rodriguez triple Junction following the representation of Patriat and Courtillot (1984) : unstable RRF model. b - Schematic isochron pattern obtained with the unstable RRF configuration of the Rodriguez Triple Junction. The isochrons are at 0.1 Ma intervals.

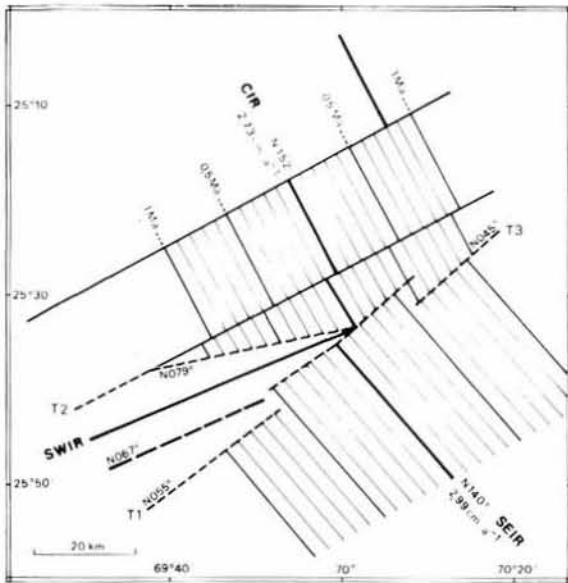


Figure 11

Schematic isochron pattern obtained with the unstable RRF configuration of the Rodriguez Triple Junction including the Jump of the triple junction. The isochrons are at 0.1 Ma intervals.

isochrons along the RTJ trace T3. The lengths of the offsets increase in the direction of the RTJ. This unstable model also predicts that the SEIR recedes at 0.18 cm a^{-1} which is a value much smaller than the 0.76 cm a^{-1} obtained with the stable model.

If the isochron pattern produced by the unstable model (Figure 10b) is superimposed on the morphostructural map (Figure 9), two discrepancies appear. At a distance of 10 km from the RTJ the CIR is offset 4 km to the northeast by a transform fault. The RTJ trace T1 is offset 5 km to the south, 15 km away from the RTJ; this offset occurred 0.5 Ma ago and corresponds to the end of the southern deep-valley of the SWIR (Figure 4). The northern deep-valley forms the southwestern branch of the RTJ. Thus, at the age of 0.5 Ma, the RTJ has jumped to the northwest. This jump corresponds to the creation of a 5 km long segment of the SEIR in place of a corresponding segment of the CIR. Therefore, the proposed model (Figure 11), which takes into account all of the directions and offsets in the morphotectonic map, explains two major morphologic features of the RTJ. The first morphologic observation is that the deep-valleys of the SWIR, close to the RTJ, are always offset to the north (Figure 12). The second is that the SEIR segment close to the RTJ has kept a constant length. The shortening of 0.18 cm a^{-1} is compensated by the RTJ jumps. The deep-valleys of the SWIR along the RTJ trace T1 have been mapped from the RTJ to $26^{\circ}40'S$ using the available Seabeam swaths (Figure 12). They are generally regularly spaced and, considering the 6-10 km distance between them, the successive RTJ jumps have occurred in the last 7 Ma with a periodicity of about 1 Ma. Figure 12 also shows the lengthening of the CIR and SWIR and the constant length of the SEIR. The

lengthening of the CIR and SWIR is accompanied by the creation of transform faults (Sclater *et al.*, 1981). Along the SWIR there is no evidence that these transform faults are linked to the evolution of the RTJ. On the contrary the transform faults along the CIR appear to be linked to the RTJ jumps. When the RTJ jumps to the northwest, the axis of the CIR, close to the RTJ, could be offset to the southwest, and creating in the process a new segment of the CIR. Unfortunately, the available profiles along the CIR are too scarce to define this mechanism in adequate detail.

The proposed unstable model has a configuration similar to a ridge-ridge-transform fault (RRF) junction. However the lengthening of the active part of the transform fault (0.14 cm a^{-1}) implies that the triple junction changes its geometry as a function of time which corresponds to the instability. The RRF configuration was rejected by Tapscott *et al.* (1980). Patriat and Courtillot (1984) have suggested, on the other hand, that the RTJ evolves in two preferred modes: "the effusive and tectonic modes, corresponding to RRR and RRF configurations respectively. These modes apparently alternate in episodes of typically 1 Ma duration". In fact, we find that the evolution of the RTJ is similar to an unstable RRF mode with episodic (1 Ma) jumps of the triple junction. The unstable RRF could correspond to the effusive mode and the jumps to the tectonic mode. In this case the duration of the tectonic mode appears much shorter than the duration of the effusive mode.

DISCUSSION AND CONCLUSIONS

The detailed maps of the RTJ yield accurate values for the directions and spreading rates of the SEIR and CIR, the directions of the traces of the RTJ and the direction of the SWIR deep-valleys. A stable RRR model for the evolution of the RTJ cannot account for these observations. This is surprising because the RTJ has remained RRR regionally since the Late Cretaceous (Tapscott *et al.*, 1980; Schlich, 1982; Patriat, 1983). Our interpretation shows that the evolution of the RTJ from 0 to 1 Ma is not a simple geometrical RRR evolution. The proposed unstable RRF model (Figure 10a and 11), is consistent with all the directions and the velocities observed. The instability, expressed by an offset of the SEIR and CIR propagating at a velocity of 0.14 cm a^{-1} , is compensated by jumps of the triple junction, which create new segments on the CIR and restore the regionally RRR triple junction. This shows that the RTJ can be regionally regarded as a stable RRR junction. However, at a more detailed scale, its evolution since 80 Ma appears more complicated and seems to be governed by two major constraints. The first constraint is that the segment of the SEIR which is close to the RTJ keeps a constant length: when the SEIR segment has shortened by several kilometers, the RTJ jumps to the northwest. This jump restores the initial length of the SEIR. The second constraint is that the SEIR and CIR

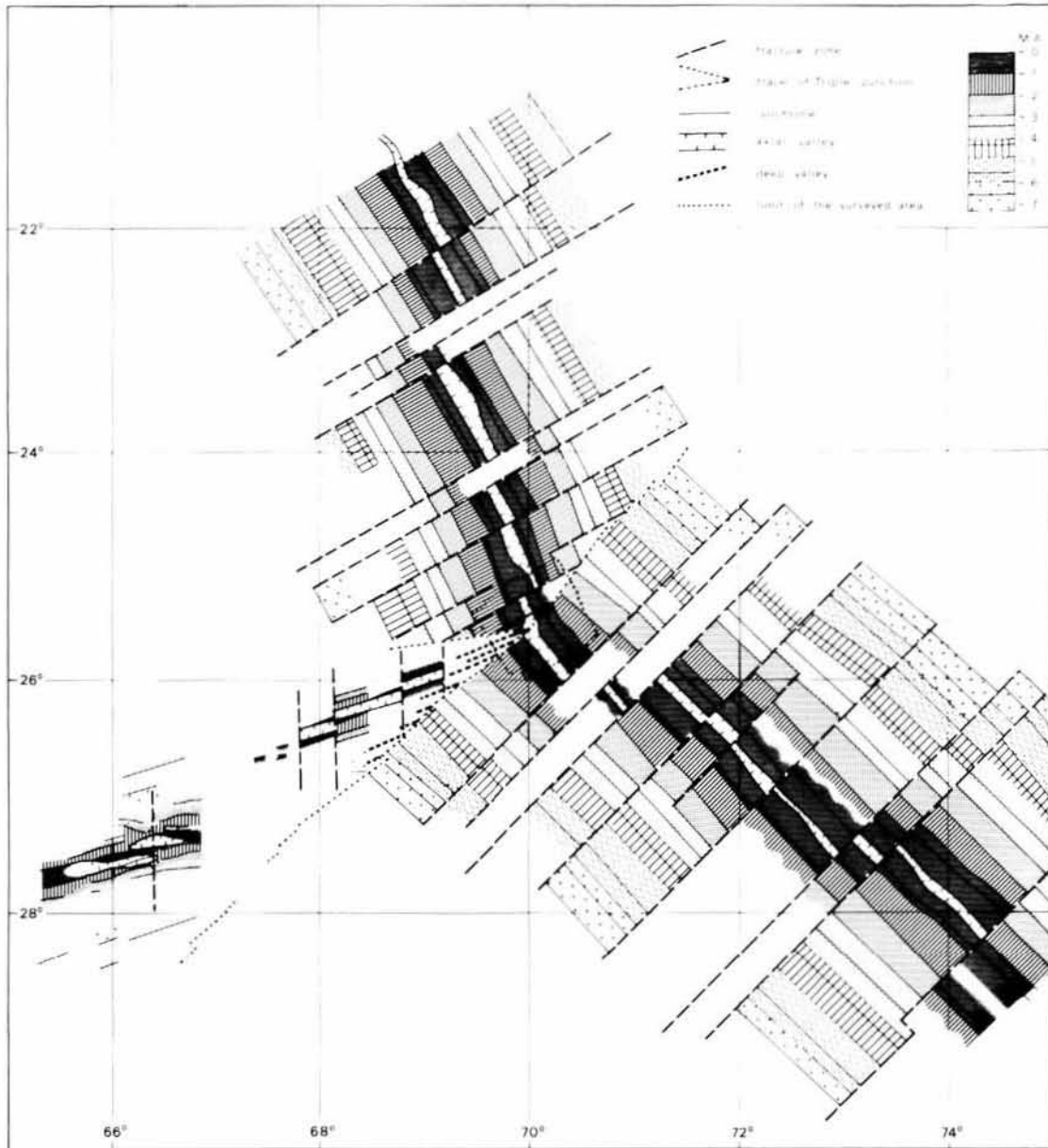


Figure 12
 Fracture zones and magnetic lineations in the vicinity of the Rodriguez Triple Junction.

are not offset by more than several kilometers, which induces ridge jumps along the CIR. These offsets are clearly seen on the RTJ trace *T3* (Figure 12) from 0 to 6 Ma. Close to the RTJ the SWIR is expressed by deep-valleys; moreover, the half spreading rate of 0.65 cm a^{-1} obtained with the models is very low and no magnetic anomalies are readable. Thus in the vicinity of the RTJ the SWIR appears to be a stretched area of the SEIR and CIR southwestern flanks, and the neovolcanic zone, defined as the zone of recent and ongoing volcanism (Macdonald, 1982) does not exist in this area.

Three other regionally RRR junctions have been surveyed in some detail : the Bouvet Triple Junction (BTJ), located in the South Atlantic Ocean ($54^{\circ}59'S$ and $00^{\circ}40'W$), has a predominantly RFF configuration (Sclater *et al.*, 1976);

the Azores Triple Junction (ATJ), located in the Central Atlantic Ocean ($39^{\circ}30'N$ and $29^{\circ}45'E$), has a regionally RRR configuration (Searle, 1980); the Galapagos Triple Junction (GTJ), located in the East Pacific Ocean ($2^{\circ}18'N$ and $101^{\circ}50'-102^{\circ}05'W$), has also a regionally RRR configuration (Searle and Francheteau, 1986). While the BTJ appears rather different, the other triple junctions are quite similar (Figure 13). The GTJ, RTJ and ATJ have two arms with similar directions and half spreading rates, while the third arm spreads at a slower rate and is at about right angles to the other two. This consistent pattern is all the more interesting as the two principal arms of the triple junctions spread with various half rates : the GTJ corresponds to a fast (spreading rate) triple junction, the RTJ to an intermediate triple junction and the ATJ to a slow triple junction. We suggest that this similarity reflects the

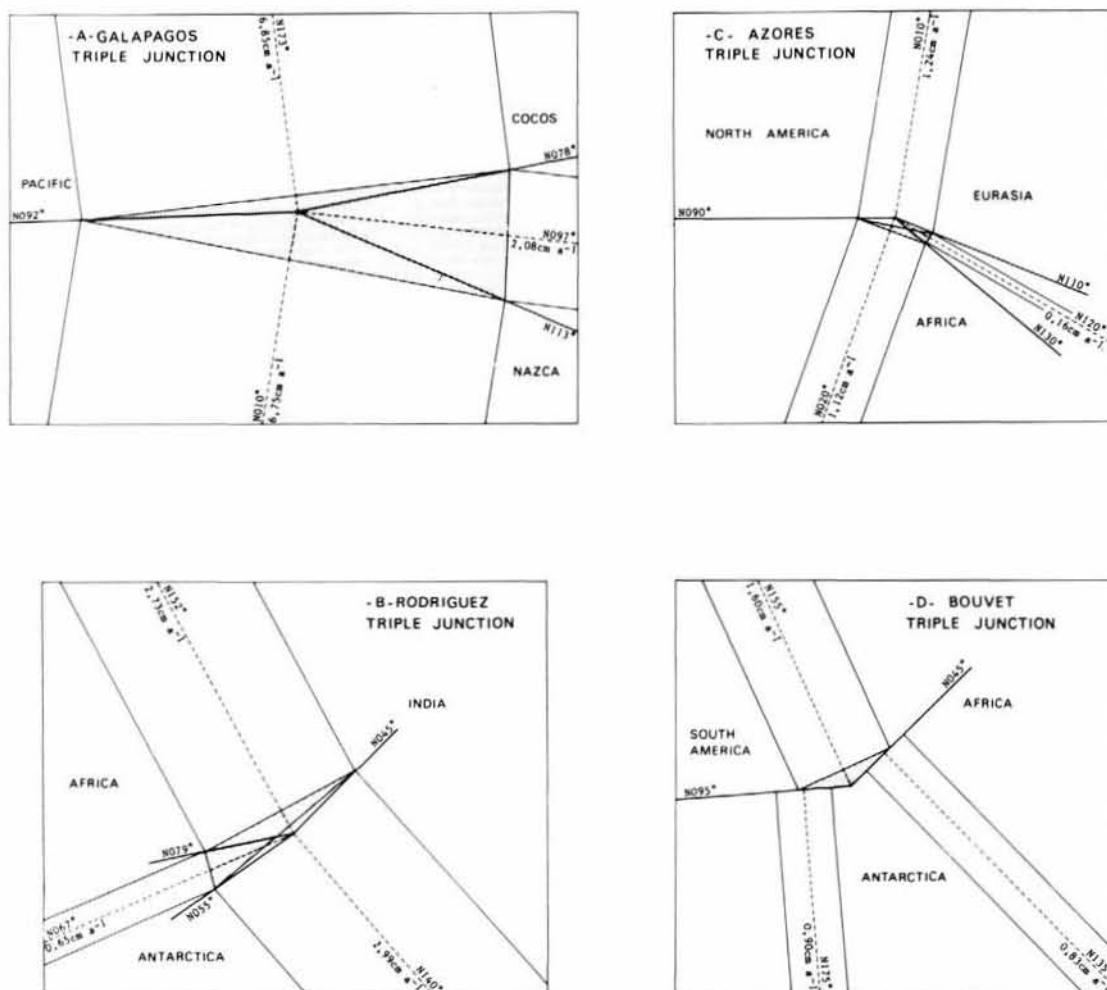


Figure 13

Present velocity triangle for triple junctions using the method of Patriat and Courtillot (1984) : (A) Galapagos Triple Junction (Searle and Francheteau, 1986); (B) Rodriguez Triple Junction (this paper); (C) Azores Triple Junction (Searle, 1980); (D) Bouvet Triple Junction (Sclater et al., 1976).

presence of continuous magma chambers beneath some ridge segments : the two faster-spreading arms of the triple junctions have connected magma chambers. The slower-spreading arm correspond to a stretched area without axial neovolcanic zone.

Acknowledgments

We thank the captain and crew of the R/V *Jean Charcot*, Rodriguez cruise, as well as our colleagues who partici-

pated to the survey and to the data processing. We thank Dr. Y. Rotstein, Dr. J. M. Marthelot and Dr. L. M. Parson for critical review of the manuscript. This research was supported by Institut Français de Recherche pour l'Exploitation de la Mer (IFREMER), Centre national de la Recherche Scientifique (ATP Océan), and Institut National des Sciences de l'Univers (INSU).

REFERENCES

Atwater T. and J. D. Mulie, 1973. Detailed Near-Bottom Geophysical Study of the Gorda Rise, *J. Geophys. Res.* **78**, 8665-8668.
 Fisher R.L., J.G. Sclater and D. P. McKenzie, 1971. Evolution of the Central Indian Ridge, Western Indian Ocean, *Geol. Soc. Amer. Bull.* **82**, 553-562.
 Lowrie W. and W. Alvarez, 1981. One Hundred Million Years of Geomagnetic Polarity History, *Geology*, **9**, 392-397.
 Macdonald K.C., 1982. Mid-Ocean Ridges : Fine Scale Tectonic, Volcanic, and Hydrothermal Processes within the Plate Boundary Zone, *Ann. Rev. Earth Planet. Sci.* **10**, 155-190.

- Macdonald K.C., S.P. Miller, S.P. Huestis and F.N. Spiess, 1980. Three-Dimensional Modelling of a Magnetic Reversal Boundary from Inversion of Deep-Tow Measurements, *J. Geophys. Res.*, **85**, 3670-3680.
- McKenzie D.P. and W.J. Morgan, 1969. Evolution of Triple Junctions, *Nature* **224**, 295-315.
- McKenzie D.P. and J.G. Sclater, 1971. The Evolution of the Indian Ocean since the Late Cretaceous, *Geophys. J. R. Astr. Soc.* **25**, 437-528.
- McKenzie M., 1987. Etude géophysique détaillée du point triple de Rodriguez et de la zone axiale des trois dorsales associées, *Thèse de Doctorat, Univ. L. Pasteur, Strasbourg I.*
- Parker R.L. and S.P. Huestis, 1974. The Inversion of magnetic anomalies in the Presence of Topography, *J. Geophys. Res.* **79**, 1587-1593.
- Patriat P., 1983. Evolution du système de dorsales de l'océan Indien, *Thèse Doct. es Sciences, Univ. Curie, Paris.*
- Patriat P. and V. Courtillot, 1984. On the Stability of Triple Junctions and its Relation to Episodicity in Spreading, *Tectonics*, **3**, 317-332.
- Peddie N.W., 1982. International Geomagnetic Reference Field, 1980; a Report by IAGA Division I Working Group 1, *Geophys. J. R. Astr. Soc.* **68**, 265-268.
- Renard V. et J.P. Allenou, 1979. Le sea-beam sondeur à multi-faisceaux du N/O «Jean Charcot»; description, évaluation et premiers résultats, *Rev. Hydrog. Intern., Monaco* **56**, 35-71.
- Royer J.Y., 1985. Evolution cinématique détaillée de la dorsale est-indienne entre le point triple de Rodriguez et les îles Saint Paul et Amsterdam, *Thèse de Doctorat, Univ. L. Pasteur, Strasbourg I.*
- Sander E.L. and C.P. Mrazek, 1982. Regression Technique to Remove Temporal Variation from Geomagnetic Survey Data, *Geophysics* **47**, 1437-1443.
- Schlich R., 1982. The Indian Ocean : Aseismic Ridges, Spreading centers, and Oceanic Basins, Nairn, A. E. M., and Stehli F.G. (eds.), *The Ocean basins and margins*, **6**, The Indian Ocean, New York Plenum Press, 51-147.
- Schlich R., M. Munsch, J.M. Marthelot, J.Y. Royer and M. Schaming, 1987. Les campagnes du N.O. Jean Charcot sur le point triple de Rodriguez (océan Indien) : premiers résultats, *Bull. Soc. Géol. France* **3**, 693-697.
- Schlich R., M. Munsch and M. Blanck, 1988. Cartes Bathymétriques, gravimétriques et magnétiques au 1/2000.000 et 1/100.000 du point triple de Rodriguez et de la zone axiale des trois dorsales associées (océan Indien), *Institut de Physique du Globe, Strasbourg, France.*
- Sclater J.G., C. Bowin, R. Hey, H. Hoskins, J. Peirce, J. Phillips and C. Tapscott, 1976. The Bouvet Triple Junction, *J. Geophys. Res.* **81**, 1857-1869.
- Sclater J.G., R.L. Fischer, P. Patriat, C. Tapscott and B. Parsons, 1981. Eocene to Recent Development of the Southwest Indian Ridge, a Consequence of the Evolution of the Indian Ocean Triple Junction, *Geophys. J. R. Astr. Soc.* **64**, 587-604.
- Searle R., 1980. Tectonic Pattern of the Azores Spreading Center and Triple Junction, *Earth Planet Sci. Lett.* **51**, 415-434.
- Searle R. and J. Francheteau, 1986. Morphology and Tectonics of the Galapagos Triple Junction, *Mar. Geophys. Res.* **8**, 95-129.
- Tapscott C.R., P. Patriat, R.L. Fisher, J.G. Sclater, H. Hoskins and B. Parsons, 1980. The Indian Ocean Triple Junction, *J. Geophys. Res.* **85**, 4723-4739.
- Weissel J.K. and D.E. Hayes, 1972. Magnetic Anomalies in the Southeast Indian Ocean, in D. E. Hayes, (ed.), *Antarctic Oceanology II : The Australian-New Zealand Sector*, *Antarctic Res. Ser.* **19**, AGU, Washington, D.C., 165-196.